EBioMedicine 46 (2019) 342–355

Contents lists available at ScienceDirect

EBioMedicine

journal homepage: www.ebiomedicine.com

EBioMedicine
Published by THE LANCET

Research paper

Age-related metabolic changes limit efficacy of deoxynucleoside-based therapy in thymidine kinase 2-deficient mice

Cora Blázquez-Bermejo [a,b], David Molina-Granada [a,b], Ferran Vila-Julià [a,b], Daniel Jiménez-Heis [a], Xiaoshan Zhou [c], Javier Torres-Torronteras [a,b], Anna Karlsson [c], Ramon Martí [a,b], Yolanda Cámara [a,b,*]

[a] Research Group on Neuromuscular and Mitochondrial Disorders, Vall d'Hebron Institut de Recerca, Universitat Autònoma de Barcelona, Barcelona, Spain
[b] Biomedical Network Research Centre on Rare Diseases (CIBERER), Instituto de Salud Carlos III, Madrid, Spain
[c] Division of Clinical Microbiology, Department of Laboratory Medicine, Karolinska Institute, Karolinska University Hospital, 141 86 Stockholm, Sweden

ARTICLE INFO

Article history:
Received 4 June 2019
Received in revised form 5 July 2019
Accepted 15 July 2019
Available online 24 July 2019

Keywords:
TK2
Deoxynucleoside therapy
mtDNA depletion
Encephalomyopathy
Thymidine
Deoxycytidine

ABSTRACT

Background: Thymidine kinase 2 (TK2) catalyses the phosphorylation of deoxythymidine (dThd) and deoxycytidine (dCtd) within mitochondria. TK2 deficiency leads to mtDNA depletion or accumulation of multiple deletions. In patients, *TK2* mutations typically manifest as a rapidly progressive myopathy with infantile onset, leading to respiratory insufficiency and encephalopathy in the most severe clinical presentations. TK2-deficient mice develop the most severe form of the disease and die at average postnatal day 16. dThd+dCtd administration delayed disease progression and expanded lifespan of a knockin murine model of the disease.

Methods: We daily administered TK2 knockout mice ($Tk2^{KO}$) from postnatal day 4 with equimolar doses of dThd +dCtd, dTMP+dCMP, dThd alone or dCtd alone. We monitored body weight and survival and studied different variables at 12 or 29 days of age. We determined metabolite levels in plasma and target tissues, mtDNA copy number in tissues, and the expression and activities of enzymes with a relevant role in mitochondrial dNTP anabolism or catabolism.

Findings: dThd+dCtd treatment extended average lifespan of $Tk2^{KO}$ mice from 16 to 34 days, attenuated growth retardation, and rescued mtDNA depletion in skeletal muscle and other target tissues of 12-day-old mice, except in brain. However, the treatment was ineffective in 29-day-old mice that still died prematurely. Bioavailability of dThd and dCtd markedly decreased during mouse development. Activity of enzymes catabolizing dThd and dCtd increased with age in small intestine. Conversely, the activity of the anabolic enzymes decreased in target tissues during mouse development. We also found that administration of dThd alone had the same impact on survival to that of dThd+dCtd, whereas dCtd alone had no influence on lifespan.

Interpretation: dThd+dCtd treatment recruits alternative cytosolic salvage pathways for dNTP synthesis, suggesting that this therapy would be of benefit for any *Tk2* mutation. dThd accounts for the therapeutic effect of the combined treatment in mice. During the first weeks after birth, mice experience marked tissue-specific metabolic regulations and ontogenetic changes in dNTP metabolism-related enzymes that limit therapeutic efficacy to early developmental stages.

Fund: This study was funded by grants from the Spanish Ministry of Industry, Economy and Competitiveness, the Spanish Instituto de Salud Carlos III, the Fundación Inocente, Inocente, AFM Téléthon and the Generalitat de Catalunya. The disclosed funders had no role in study design, data collection and analysis, decision to publish, or preparation of the manuscript.

1. Introduction

Thymidine kinase 2 (TK2), a mitochondrial enzyme encoded by nuclear DNA, catalyses a limiting step in mitochondrial deoxynucleoside (dN) salvage. This pathway recycles dNs from endogenous metabolism and diet by using a set of kinases that catalyse equivalent reactions in the cytosol and mitochondria. TK2 phosphorylates the pyrimidine dNs, deoxythymidine (dThd) and deoxycytidine (dCtd), to deoxythymidine monophosphate (dTMP) and deoxycytidine monophosphate (dCMP), respectively. These deoxynucleoside monophosphates (dNMPs) are consecutively phosphorylated to deoxynucleoside triphosphates

Abbreviations: CDA, cytidine deaminase; CNS, central nervous system; dCK, deoxycytidine kinase; dCMP, deoxycytidine monophosphate; dCtd, deoxycytidine; dN, deoxynucleoside; dNMP, deoxynucleoside monophosphate; dNTP, deoxynucleoside triphosphate; dThd, deoxythymidine; dTMP, deoxythymidine monophosphate; KO, knockout; mtDNA, mitochondrial DNA; nDNA, nuclear DNA; PBS, phosphate buffered saline; Thy, thymine; TK1, thymidine kinase 1; TK2, thymidine kinase 2; TP, thymidine phosphorylase; *Tymp*, thymidine phosphorylase gene; WT, wild-type.

* Corresponding author at: Laboratori de Patologia Neuromuscular i Mitocondrial, Institut de Recerca Hospital Universitari Vall d'Hebron-CIBERER, Passeig Vall d'Hebron, 119-129, 08035 Barcelona, Spain.
E-mail address: yolanda.camara@vhir.org (Y. Cámara).

https://doi.org/10.1016/j.ebiom.2019.07.042

Research in context

Evidence before this study

Thymidine kinase 2 (TK2) is a key enzyme for mitochondrial pyrimidine dNTP synthesis. Mutations in TK2 reduce availability of dTTP and dCTP and interfere with normal mitochondrial DNA (mtDNA) replication leading typically to a severe and rapidly-progressive myopathy. Supplementation with precursors in the form of deoxynucleosides (dNs), specifically deoxythymidine (dThd) and deoxycytidine (dCtd), activates the synthesis of dTTP and dCTP through alternative enzyme pathways and effectively counteracts the defect in a knockin mouse model of the disease.
These results prompted the compassionate use of dThd plus dCtd for the treatment of patients suffering TK2 deficiency with significant positive results so far.

Added value of this study

Here, we use an alternative mouse model completely devoid of TK2 activity (knockout mouse) with a fatal encephalomyopathy phenotype, similar to that observed for the knockin mice. We confirm that administration of dThd + dCtd, delays disease progression, doubles life expectancy and counteracts mtDNA depletion in most target tissues of young knockout mice. In addition, we observe how administration of dThd alone leads to the same therapeutic effect in terms of survival. However, important tissue-specific metabolic regulations predict different outcomes for the combined or individual therapy depending on the target tissue.
Both TK2-deficient mouse models die prematurely in spite of the treatment. In this study, we deeply characterize metabolic response to dNs-treatment, and identify decreased activity of salvage kinases and increased deoxynucleoside catabolism as key factors limiting therapeutic efficacy to early developmental stages in mice.

Implications of all the available evidence

No effective therapeutic option was available for TK2 deficient patients before dTMP and dCMP were proposed, followed by the observation that the active compounds in this treatment are dThd and dCtd. In the most severe cases, TK2-deficient patients die during early infancy. After recent experience of compassionate use of dThd and dCtd in TK2 deficiency, a cohort of patients is being treated with positive effects on survival, motor and respiratory function. Hence, it is at the utmost importance to understand how dThd and dCtd exert their metabolic effect and what factors may be lessening their therapeutic potential.
Our study will be crucial for the design of a next-coming clinical trial for TK2-deficiency treatment and will surely be of interest in expanding dN-based therapies for the treatment of other mitochondrial DNA depletion syndromes.

(dNTPs) and incorporated into mitochondrial DNA (mtDNA) during replication [32] (Fig. 1). Thus, mutations in *TK2* result in mitochondrial deoxythymidine triphosphate (dTTP) and deoxycytidine triphosphate (dCTP) insufficiency, dNTP pool imbalance, and consequent mtDNA depletion or accumulation of multiple mtDNA deletions [2,11,26,29].

The clinical presentation of TK2 deficiency is mainly myopathic. Based on the age at onset and severity, patients can be classified into three main groups, from the most severe and common to the milder and less frequent manifestations: 1) infantile-onset myopathy with occasional neurological involvement, severe mtDNA depletion, and early death; 2) childhood-onset myopathy with mtDNA depletion and moderate to severe progression of weakness; and 3) late-onset myopathy

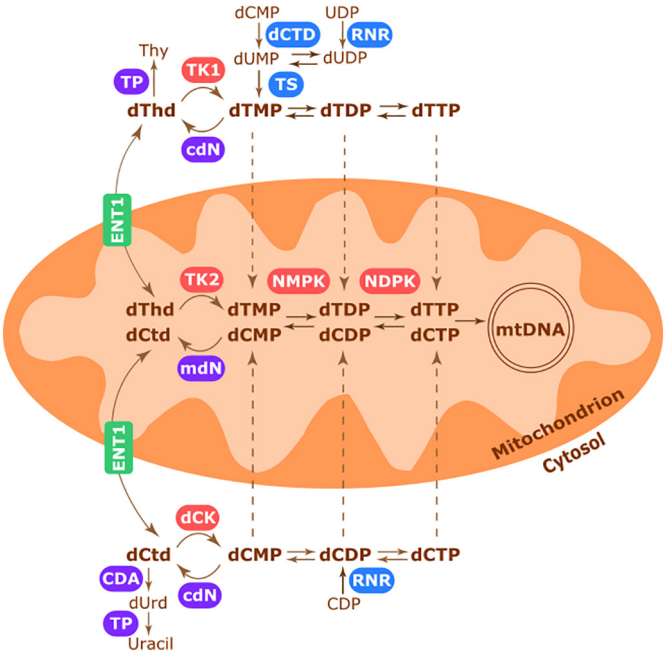

Fig. 1. Schematic representation of the main enzyme pathways involved in mitochondrial pyrimidine dNTPs metabolism. Proteins involved in the de novo synthesis pathway are depicted in blue. Kinases involved in the deoxynucleoside salvage pathway are depicted in red. Enzymes participating in catabolism of dNs are depicted in purple. Nucleoside transporters from cytosol to mitochondria are represented in green. Abbreviations: CDA, cytidine deaminase; cdN, cytosolic deoxyribonucleotidase; dCTD, dCMP deaminase; dCK, deoxycytidine kinase; ENT1, equilibrative nucleoside transporter 1; mdN, mitochondrial deoxyribonucleotidase; NDPK, nucleotide diphosphate kinase; NMPK, nucleotide monophosphate kinase; TK1, thymidine kinase 1; TK2, thymidine kinase 2; TP, thymidine phosphorylase; TS, thymidylate synthase; RNR, ribonucleotide reductase.

with mild limb weakness and slow progression to respiratory insufficiency [11].

Two different TK2-deficient mouse models have been generated to investigate the molecular mechanism of this disease, a knockin model for a common pathogenic mutation, p.His121Asn in humans (p.His126Asn in mice) [1], and a knockout mouse [34]. In patients, TK2 deficiency predominantly causes myopathy, but both mouse models manifest major central nervous system (CNS) involvement, with development of fatal encephalomyopathy resembling the most severe cases of the disease in humans [11,12].

Therapies designed to feed dN salvage have proven to delay disease progression and increase survival. The first pre-clinical studies on the knockin model intended to bypass the TK2 defect with administration of dTMP and dCMP. This treatment augmented mtDNA levels in the target tissues and prolonged survival with dose-related efficacy, although phenotype rescue was incomplete and mice still died prematurely before adulthood [10]. Based on these results, dNMPs were first used to treat a few patients [6]. Later studies identified dNs as the active agents following dNMPs administration. dNMPs are charged compounds and in the absence of a known transporter, they cannot be internalized by cells. In addition, dNMPs are rapidly dephosphorylated to dNs in vivo by nucleotidases and phosphatases [4,35]. In a later study using the same mouse model, López et al. found that co-administration of dThd and dCtd yielded similar results [16]. These positive data served as a proof-of-concept that dNs could be effective therapeutic agents for TK2 deficiency, and prompted their use as compassionate therapy. So far, the treatment has provided clinically significant benefits, especially in infantile- and childhood-onset cases, and has led to improvement or stabilization of respiratory function in late-onset cases after a few years or even months of therapy [6].

Despite the promising pre-clinical results, dN-treated mice still die prematurely [16]. As there is no currently available alternative therapy for patients with TK2 deficiency, it is crucial to determine what elements may act to lessen the efficacy of dNs. Here, using the knockout model generated by Zhou et al. [34], we perform a deep analysis of the mechanisms regulating dNTP homeostasis and identify factors that should be key for leveraging the therapeutic potential of dNs.

2. Materials and methods

2.1. Ethics statement

This study was conducted in accordance with the rules established by the Generalitat de Catalunya for the Care and Use of Laboratory Animals. The protocol was approved by the Ethics Committee for Animal Experimentation of the Vall d'Hebron Research Institute (Permit Number: 02/17).

2.2. Mice housing, treatment administration, tissue collection and endpoints

The study was carried out with *TK2* knockout mice ($Tk2^{KO}$) (C57BL/6 genetic background) previously generated and characterized as described [34]. Mice were housed and bred in a standard controlled environment under a 12-h light-dark cycle with ad libitum access to water and regular rodent chow diet. $Tk2^{KO}$ mice develop a fatal encephalomyopathy and die at around two weeks of age. We monitored body weight, general behaviour and appearance, and survival on a daily basis. For ethical reasons, we euthanized mice in the survival studies when they were too weak to move in the cage and thereby obtain necessary food and drink.

Treatment was administered daily by single-dose oral gavage starting from postnatal day 4. Solutions of dThd, dCtd, dTMP, and dCMP were prepared in PBS, filter-sterilized, and stored at 4 °C (−20 °C for long-term storage) until administered to $Tk2^{KO}$ mice and wild-type littermates ($Tk2^{WT}$). dThd and dCtd were administered, either combined or individually, each at a dose of 400 mg/kg/day (165 mM dThd and 176 mM dCtd), whereas dTMP and dCMP were co-administered at an equimolar dose of 620 mg/kg/day. A group of control mice was administered PBS solution (vehicle).

Mice were sacrificed at 12 or 29 days of age (except those included in the survival analysis) 1 h after treatment administration (coinciding with maximum bioavailability of the administered treatments in blood, as assessed in our preliminary pharmacokinetic studies). The health status of treated $Tk2^{KO}$ mice degenerated gradually, showing the first signs of weakness a few days before death. Hence, to prevent dehydration and malnutrition at early stages of the disease, we provided all litters with accessible semi-solid food from day 15.

Circulating peripheral blood (mice at 12 days of age) or cardiac puncture blood (mice at 29 days of age) was collected in EDTA (Microvette capillary tubes, SARSTEDT) and processed (3500 g at 4 °C for 5 min) to obtain plasma. Samples were stored at −20 °C until further use. Tissues (brain, liver, and skeletal muscle [gastrocnemius]) were collected, immediately frozen in liquid nitrogen and stored at −80 °C until further use. The small intestine lumen was cleansed with abundant saline solution prior to freezing in liquid nitrogen.

2.3. mtDNA copy number determination

Total DNA was isolated from frozen tissues ground in liquid nitrogen (QIAamp DNA Mini Kit, Qiagen) and dissolved in 10 mM Tris-HCl (pH 8). For each sample, 1:3 dilutions and duplicates were assessed. Quantitative real-time PCR reactions were performed in 384-well plates using the TaqMan Universal PCR Master Mix II, with UNG (Applied Biosystems). Custom-designed sets of TaqMan primers and probes were used for relative mtDNA (*16S rRNA* gene [30]) versus nDNA (*angiogenin 1* [*Ang1*, Mm00833184_s1] single copy gene) copy number quantification. Two different standard curves with cloned *16S rRNA* and *Ang1* amplicons were used for absolute quantification of mtDNA and nDNA. Detection was done using an ABI PRISM 7900HT Sequence Detection System (Applied Biosystems).

2.4. Determination of metabolite levels in mouse plasma and tissues

dThd, dCtd, and their degradation products (thymine [Thy] and deoxyuridine [dUrd], respectively) were measured in plasma and tissue samples by liquid chromatography coupled to tandem mass spectrometry (LC-MS/MS), using an LC-MS/MS system (Acquity UPLC-XevoTM TQ Mass Spectrometer, Waters, Milford, MA, USA). Frozen tissues were ground in liquid nitrogen and homogenized in lysis buffer (50 mM Tris-HCl, pH 7.2; 1% Triton X-100; 2 mM phenylmethylsulfonyl fluoride; 0.02% 2-mercaptoethanol; 100 μM tetrahydrouridine (THU); and 100 μM 6-amino-5-bromouracile [6A5BrU]) by mechanical disruption using a plastic pestle. Deuterated dThd (1 μM; Cambridge Isotope Laboratories) was used as an internal standard. Homogenates were centrifuged at 20,000*g* at 4 °C for 30 min, and supernatants were collected. Protein concentration was measured by the Bradford method. Diluted plasma and tissue homogenates were deproteinised by ultrafiltration (10 kDa Amicon Ultra filters, Millipore) at 14,000 g at 4 °C for 30 min and stored at 20 °C until further use. Samples and standards were loaded into 96-well plates for injection in the LC-MS/MS system. For all determinations, the stationary phase was an Acquity UPLC BEH C18 column (100 × 2.1 mm, 130 Å pore, 1.7 mm particle, Waters). For determinations, 7.5 μl of sample was injected into the LC-MS/MS system and resolved at 0.5 ml/min through a binary gradient elution using a saline buffer (20 mM ammonium acetate, pH 5.6) and acetonitrile as follows: time 0–1.1 min, isocratic 100% saline buffer; 1.1–5 min, gradient from 0 to 13.6% acetonitrile; 5–5.1 min, gradient from 13.6 to 100% acetonitrile; 5.1–6.1 min, isocratic 100% acetonitrile; and 6.1–7.2 min, isocratic 100% saline buffer. Detection of the eluate components was performed using multiple reaction monitoring, in positive electrospray mode with the following *m/z* transitions: 255.0 > 133.8 (deuterated dThd), 242.8 > 127.1 (dThd), 228.8 > 113.1 (dUrd), 227.9 > 112.1 (dCtd), and 126.7 > 110.0 (Thy). Identification of all compounds was based on the retention time and specific ion transitions. Calibration curves made with aqueous multistandards were processed in parallel, and concentrations were obtained from interpolation of the peak areas using TargetLynx software (Waters).

2.5. RNA isolation and analysis of expression

RNA was isolated from frozen tissues ground in liquid nitrogen with TRIzol Reagent (Invitrogen), resuspended in RNAase-free water, and quantified using a NanoDrop spectrophotometer. A 5-μg amount of RNA was treated with DNaseI (Ambion DNAse-free) and reverse transcribed to cDNA by using the High-Capacity cDNA Archive Kit (Applied Biosystems). Quantitative real-time PCR reactions were carried out in 384-well plates with TaqMan Universal PCR Master Mix II, with UNG (Applied Biosystems). Predesigned TaqMan Gene Expression Assays (Applied Biosystems) were used for detection of thymidine phosphorylase (*Tymp;* Mm01301808_m1), cytidine deaminase (*Cda,* Mm01341706_m1), thymidine kinase 1 (*Tk1,* Mm01246403_g1) and deoxycytidine kinase (*Dck,* Mm00432794_m1) mRNA. Each sample was analysed in triplicate, and the average value was used as the mRNA measure. mRNA levels of cyclophilin A (*Ppia;* Mm02342430_g1) were used as the reference for normalization among samples.

2.6. Enzyme activity determinations

Catabolic activities thymidine phosphorylase (TP) and cytidine deaminase (CDA) were adapted from Martí et al. [19]. Briefly, frozen tissues were ground in liquid nitrogen and homogenized in lysis buffer

(50 mM Tris-HCl, pH 7.2; 1% Triton X-100; 2 mM phenylmethylsulfonyl fluoride [PMSF]; 0.02% 2-mercaptoethanol) by mechanical disruption with a plastic pestle. Homogenates were centrifuged at 20,000*g* at 4 °C for 30 min, and supernatants collected for protein concentration determination by the Bradford method. A 100-μg amount of protein was incubated at 37 °C for 1 h with 10 mM dThd in a total volume of 100 μl reaction buffer (0.1 M Tris-arsenate, pH 6.5) for TP activity or with 5 mM dCtd in a total volume of 100 μl reaction buffer (0.2 M Tris-HCl, pH 8; 100 μM 6-amino-5-bromouracile [6A5BrU]) for CDA activity. A blank in which dThd or dCtd was omitted, was also processed for each sample. The reaction was stopped by addition of 1 ml of 0.55 M HCl to all samples and 10 mM dThd or dCtd to all blanks. Samples were centrifuged at 20,000*g* at 4 °C for 10 min. Supernatants were injected into an Acquity UPLC system (Waters, Milford, MA, USA), and eluted at 0.5 ml·min-1 with a saline buffer eluent (20 mM ammonium acetate, pH 5.6) and an organic eluent (methanol gradient grade), according to the following gradient: time 0–1.1 min, isocratic 100% saline buffer; 1.1–5 min, gradient from 0 to 13.6% methanol; 5–5.1 min, gradient from 13.6 to 100% methanol; 5.1–6.1 min, isocratic 100% methanol; and 6.1–7.2 min, isocratic 100% saline buffer. The column used was an Acquity UPLC BEH C18 column (100 × 2.1 mm, 130 Å pore size, 1.7 μm particle size [Waters]). Eluate absorbance was monitored at 267 nm, and the Thy (product of TP reaction) or dUrd (product of CDA reaction) peaks were identified and quantified using a multistandard calibration curve.

Anabolic activities thymidine kinase 1 (TK1) and deoxycytidine kinase (dCK) were measured using a radiochemical method [24]. Briefly, tissue homogenates were prepared as for TP and CDA determinations in lysis buffer (50 mM Tris-HCl, pH 7.2; 1% Triton X-100; 2 mM PMSF; 0.02% 2-mercaptoethanol). Homogenates were centrifuged at 20,000*g* for 30 min at 4 °C, and supernatants collected for protein concentration determination by the Bradford method. A 120-μg amount of extract was incubated for 1 h at 37 °C in a reaction buffer (50 mM Tris-HCl, pH 7.6; 5 mM MgCl2; 5 mM ATP; 10 mM NaF; 2 mM DTT; 0.5 mg/ml BSA) containing appropriate [^{3}H]-labelled substrates (Moravek, Inc.) and inhibitors. For TK1 activity, 25 μM [methyl-^{3}H]-Thd, 1 mM (for brain determinations) or 100 mM (for liver determinations) dCtd, 100 μM THU, and 100 μM 6A5BrU were used. For dCK activity, 25 μM [^{3}H]-dCtd, 10 mM dThd, 100 μM THU, and 100 μM 6A5BrU were used. THU and 6A5BrU were added to prevent degradation of the substrates. As TK2 can phosphorylate both substrates and interfere with specific determination of TK1 and dCK activity, we used an excess of competitive substrates (dCtd or dThd respectively) to inhibit TK2-dependent phosphorylation in the two reactions. In preliminary assays, we determined the inhibitory capacity of competitive substrates of each enzyme and calculated the final values accordingly. After incubation, the reactions were spotted on DEAE Filtermat filters (Perkin Elmer) and left to air-dry. Filters were washed twice for 5 min in 1 mM ammonium formate, and for 5 additional min in water, and then left to air-dry. Dried filters were coated with MeltiLex scintillation wax (Perkin Elmer). The reaction product retained in the filters was detected and quantified with a MicroBeta2 system (Perkin Elmer). Results are expressed in pmols of the product (dTMP or dCMP) formed per mg of protein per min. Activity measurements were done in triplicate and quantified using a calibration curve.

2.7. Statistical analysis

Statistical analysis was performed with GraphPad Prism 6 software. The specific tests used for each assay are indicated in the Results section or the figure legends. For statistical purposes, undetectable values were considered zero. Mice sacrificed for plasma and tissue collection, or mice that died due to experimental manipulation were considered as censored observations in Kaplan-Meier statistical analyses. Detailed information on animals included in the survival study is provided in Supplementary Table 1.

2.8. Data availability

The datasets generated during the experimental procedures and analysis are available from the corresponding author on reasonable request.

3. Results

3.1. Daily administration of pyrimidine deoxynucleosides extends life expectancy of a mouse model devoid of TK2 enzyme activity

We treated *TK2* knockout (*Tk2*^{KO}) pups and wild-type littermates (*Tk2*^{WT}) with dThd plus dCtd (each at 400 mg/kg/day), an equimolar dose of the corresponding dNMPs, dTMP plus dCMP (each at 620 mg/kg/day), or phosphate buffered saline (PBS, vehicle) by daily oral gavage starting at postnatal day 4. Previous studies have shown that untreated *TK2*^{KO} mice die prematurely at around two weeks of age [34]. We obtained similar results after daily oral PBS administration. PBS-treated *Tk2*^{KO} mice exhibited pronounced weight loss starting at 14 to 15 days of age and died shortly after (median, 16 days of age; mean ± SD, 16.3 ± 2.6 days of age; $n = 20$) (Fig. 2). Treatment with either pyrimidine dNMPs (dTMP+dCMP) or the corresponding dNs (dThd +dCtd) delayed disease progression and strongly attenuated growth retardation (Fig. 2). Survival of *Tk2*^{KO} mice treated with dThd+dCtd or dTMP+dCMP was extended up to 34 or 32 (median) days of age (mean ± SD, 31.9 ± 6.9 days of age; $n = 12$; mean ± SD, 34.1 ± 6.0 days of age; $n = 11$, respectively) (Fig. 2A). There were no adverse effects in *Tk2*^{WT} littermates treated up to 41 days with either PBS or dThd+dCtd (up to 51 days with dTMP+dCMP).

These results are equivalent to those obtained with an alternative TK2-deficient model, the p.His126Asn knockin mouse, exposed to similar treatments [1,10,16].

3.2. dThd+dCtd administration rescues mtDNA copy number in skeletal muscle only at early ages

We analysed *Tk2*^{KO} mice and *Tk2*^{WT} littermates at two time-points, at 12 days of age, close to the stage when untreated or PBS-treated *Tk2*^{KO} naturally die [34], and 29 days of age, close to the maximum survival achieved with treatment. At day 12, *Tk2*^{KO} mice showed a significantly reduced mtDNA copy number in skeletal muscle (gastrocnemius), and particularly, in brain (Fig. 3). Treatment with dThd+dCtd rescued mtDNA depletion only in skeletal muscle. On day 29, we were only able to study *Tk2*^{WT} and treated *Tk2*^{KO} animals because PBS-treated *Tk2*^{KO} mice do not survive beyond 20 days of age. At this stage, mtDNA depletion was obvious in all analysed tissues of treated *Tk2*^{KO} animals (liver, brain, and skeletal muscle) with the exception of small intestine, indicating that the treatment had failed to rescue mtDNA copy number in any case.

Furthermore, dThd+dCtd treatment elevated mtDNA copy number in several tissues of *Tk2*^{WT} mice. This increase was significant at 12 days of age in liver and at 29 days in skeletal muscle (Fig. 3).

3.3. dThd and dCtd bioavailability markedly decreases during mouse development

We collected blood and tissues 1 h after dThd+dCtd administration and determined concentrations of the two dNs and their first catabolic products, thymine (Thy) and deoxyuridine (dUrd), respectively. As was expected, plasma concentrations of both dNs were significantly higher after treatment, with dCtd reaching half the levels of dThd (Fig. 4). Nevertheless, administration of the same doses of dThd+dCtd resulted in much lower plasma levels of these compounds in 29-day-old mice (mean ± SD of dThd: *Tk2*^{WT}-dThd+dCtd 40.6 ± 17.0; *Tk2*^{KO}-dThd+dCtd 25.4 ± 9.0; mean ± SD of dCtd: *Tk2*^{WT}-dThd+dCtd 7.5 ± 9.8; *Tk2*^{KO}-dThd+dCtd 2.9 ± 1.7) than in the 12-day-old littermates

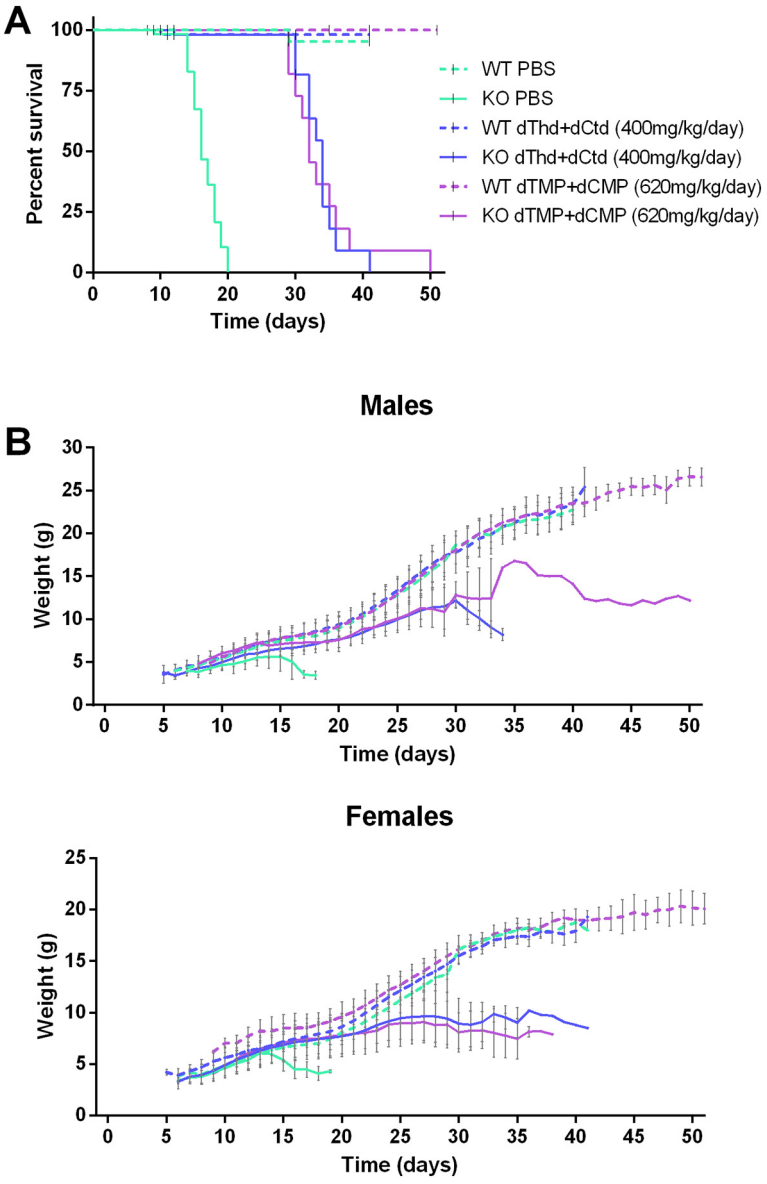

Fig. 2. Co-administration of dThd + dCtd increases life expectancy and attenuates disease progression in $Tk2^{KO}$ mice. $Tk2^{KO}$ mice (solid lines) and $Tk2^{WT}$ (dashed lines) littermates were daily administered PBS (vehicle; 10 μl/g), 400 mg/kg of dThd+dCtd, or an equimolar dose of 620 mg/kg of dTMP+dCMP. (**A**) Survival proportions, Kaplan-Meier curve ($Tk2^{WT}$-PBS, $n = 47$; $Tk2^{KO}$-PBS, $n = 58$; $Tk2^{WT}$-dThd+dCtd, $n = 55$; $Tk2^{KO}$-dThd+dCtd, $n = 48$; $Tk2^{WT}$-dTMP+dCMP, $n = 14$; $Tk2^{KO}$-dTMP+dCMP, $n = 11$. Mantel-Cox test: $Tk2^{KO}$-PBS versus $Tk2^{WT}$-PBS, $p < .001$; $Tk2^{KO}$-dThd+dCtd versus $Tk2^{KO}$-PBS, $p < .001$; $Tk2^{KO}$-dTMP+dCMP versus $Tk2^{KO}$-PBS, $p < .001$; $Tk2^{KO}$-dTMP+dCMP versus $Tk2^{KO}$-dThd+dCtd, non-significant differences). Censored observations appear as black ticks in the graph (**B**) Weight progression for female and male mice (Males: $Tk2^{WT}$-PBS, $n = 30$; $Tk2^{KO}$-PBS, $n = 32$; $Tk2^{WT}$-dThd+dCtd, $n = 40$; $Tk2^{KO}$-dThd+dCtd, $n = 36$; $Tk2^{WT}$-dTMP+dCMP, $n = 7$; $Tk2^{KO}$-dTMP+dCMP, $n = 3$. Females: $Tk2^{WT}$-PBS, $n = 30$; $Tk2^{KO}$-PBS, $n = 25$; $Tk2^{WT}$-dThd+dCtd, $n = 35$; $Tk2^{KO}$-dThd +dCtd, $n = 32$; $Tk2^{WT}$-dTMP+dCMP, $n = 7$; $Tk2^{KO}$-dTMP+dCMP, $n = 8$. Results represent mean values for each time point; error bars indicate SD).

(mean ± SD of dThd: $Tk2^{WT}$-dThd+dCtd 207.9 ± 29.3; $Tk2^{KO}$-dThd +dCtd 190.2 ± 54.5; mean ± SD of dCtd: $Tk2^{WT}$-dThd+dCtd 90.9 ± 11.2; $Tk2^{KO}$-dThd+dCtd 82.6 ± 27.1) (Fig. 3). Likewise, although the age-related differences were not as marked, we observed the same trend for Thy and dUrd plasma levels (Fig. 4).

We also determined dThd, dCtd, Thy, and dUrd levels in the 4 different tissues (brain, liver, skeletal muscle, and small intestine). Given the presence of dNs-dedicated transporters in cell membranes [33], we expected that the intracellular levels would largely mirror the concentration of these compounds in plasma. In fact, dThd+dCtd administration triggered an increase in the levels of all compounds in all tissues of 12-day-old mice analysed at only 1 h after oral administration (Fig. 5 and Supplementary Fig. 1). Again, levels of the therapeutic dNs and those of their first catabolic products were significantly lower in tissues from older animals. dThd and dCtd concentrations were particularly high in small intestine, likely due to active absorption of these compounds after oral administration (Fig. 5).

In general, we found no marked genotype-related differences, except for a trend in which dThd and dUrd concentrations were slightly lower in treated $Tk2^{KO}$ mice than in $Tk2^{WT}$ (dThd from 29d $Tk2^{WT}$-dThd+dCtd vs $Tk2^{KO}$-dThd+dCtd: plasma $p < .05$, brain and liver $p < .01$; dUrd from 29d $Tk2^{WT}$-dThd+dCtd vs $Tk2^{KO}$-dThd+dCtd: plasma and brain $p < .05$, liver $p < .01$. *P*-values obtained with the Mann-Whitney *U* test) (Figs. 4 and 5, and Supplementary Fig. 1).

3.4. Expression and activity of key metabolic enzymes undergo marked ontogenetic changes

In the absence of TK2 activity, phosphorylation of administered dThd and dCtd necessarily depends on the catalytic activity of

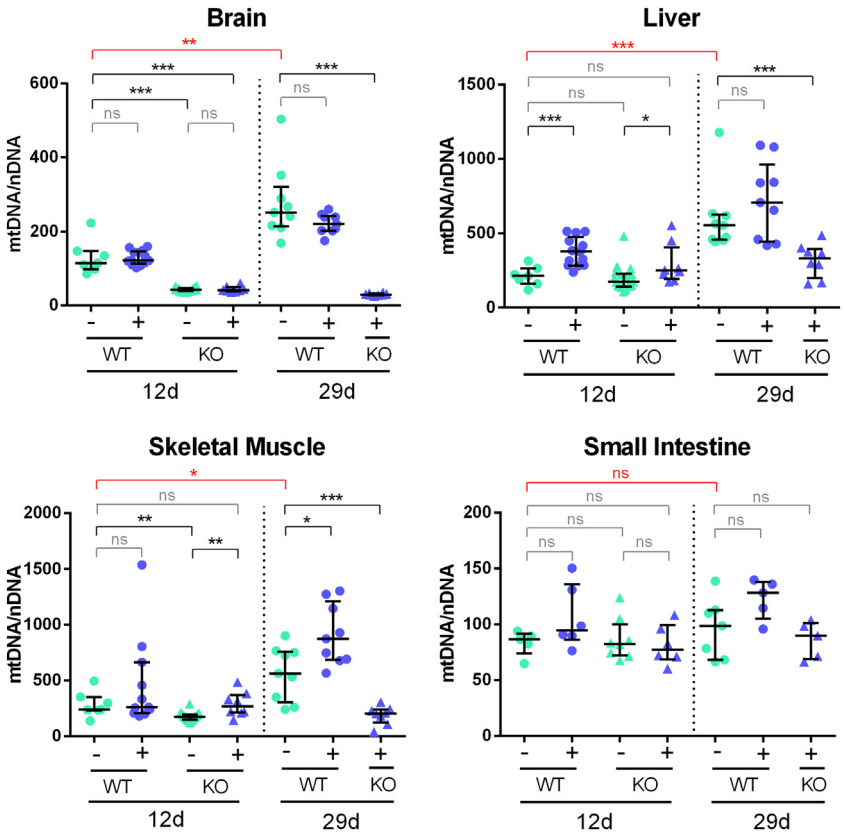

Fig. 3. Co-administration of dThd + dCtd rescues mtDNA depletion in targeted tissues of $Tk2^{KO}$ mice only at an early age. mtDNA and nDNA levels were determined by quantitative real-time PCR in mice aged 12 (12d) or 29 days (29d). Results indicate the ratio of mtDNA to nDNA in brain, liver, skeletal muscle (gastrocnemius), and small intestine of $Tk2^{KO}$ (KO; triangles) and $Tk2^{WT}$ (WT; dots) mice, treated with either 400 mg/kg/day of dThd+dCtd (+; blue) or PBS (−; green). Tissues were collected 1 h after oral gavage. Scatter plots represent the median (horizontal line) with interquartile range (mice for each group in brain, n = 7–18; liver, n = 7–18; skeletal muscle, n = 7–18 and small intestine, n = 5–8). *P*-values obtained with the Mann-Whitney *U* test: *$p < .05$; **$p < .01$; ***$p < .001$; ns, non-significant differences. Age-related statistical significance lines and *p*-values are in red.

alternative enzymes. Cytosolic deoxypyrimidine kinases, namely deoxycytidine kinase (dCK) and thymidine kinase 1 (TK1), catalyse equivalent reactions to TK2 outside mitochondria. We investigated expression of these key anabolic enzymes in tissues of PBS-treated or dThd+dCtd-treated $Tk2^{WT}$ and $Tk2^{KO}$ littermates at 12 and 29 days of age.

Downregulation of TK1 expression has already been described during normal mouse development [7]. Accordingly, we found decreased *Tk1* mRNA expression in all analysed tissues from 29-day-old mice relative to that of 12-day-old mice (except for small intestine where *Tk1* mRNA levels remained unchanged in both age groups) (Fig. 6A). Interestingly, we found that *Tk1* mRNA levels were sustained specifically in brain of treated 29-day-old $Tk2^{KO}$ mice. Because we lacked a working antibody that specifically recognized mouse TK1 protein, we were unable to determine TK1 protein levels. We also found that 12-day-old $Tk2^{KO}$-PBS mice had slightly increased (in liver) and decreased (in skeletal muscle) *Tk1* mRNA levels. However, these changes were not confirmed when TK1 enzyme activity was tested in liver and brain (Fig. 6B). In liver, TK1 activity was reduced in older animals, whereas in brain, it was particularly low already at 12 days of age.

Dck mRNA expression had decreased in liver of all 29-day-old mice regardless of their genotype, although the decrease was greater in treated $Tk2^{KO}$ mice (Fig. 6A). Enzyme activity (Fig. 6B) determinations in brain and liver correlated with steady state dCK protein levels assessed by western blot (Supplementary Figs. 2 and 3) and confirmed a considerable dCK reduction in both tissues during normal mouse development. Interestingly, this decreased was not observed in brain from $Tk2^{KO}$ mice.

An important factor that regulates the bioavailability of administered dNs is the activity of catabolic enzymes responsible for their degradation. Thymidine phosphorylase (TP) is the main enzyme catalysing degradation of dThd in humans and mice (although in the latter, dThd is also substrate for uridine phosphorylase [8]). Cytidine deaminase (CDA) is the enzyme catalysing dCtd deamination, the first step in the catabolic pathway of this dN [9]. We performed a preliminary longitudinal study of TP and CDA activities in untreated wild-type mice up to 70 days of age. Up to 30 days of age, we observed no major differences over time in brain and skeletal muscle (very low activity for both enzymes), but there was a clear increase in the activity of both enzymes in small intestine and a decrease in liver (Supplementary Fig. 4). Hence, we decided to focus on liver and small intestine for a deeper study in all treated animal groups.

We confirmed that *Tymp* mRNA expression (Fig. 7A) and TP activity (Fig. 7B), were markedly higher in small intestine of older mice. This observation is in agreement with the high Thy concentration found in intestine of 29-day-old mice (Fig. 5). CDA activity was higher than TP activity at early stages of development, but in small intestine it also increased with age. Upregulation of both TP and CDA enzyme activity and mRNA levels in small intestine suggests this tissue may be important for limiting the efficacy of orally administered dThd and dCtd.

In liver, we also observed an upregulation of *Tymp* mRNA levels (Fig. 7A) and TP activity (Fig. 7B) at 29 days of age, specifically in treated $Tk2^{KO}$ animals. Conversely, *Cda* mRNA expression (Fig. 7A) and activity (Fig. 7B) were downregulated in liver from older mice. Some genotype-related changes in *Cda* mRNA expression were also revealed with either increases (in brain) or decreases (in skeletal muscle), specifically in 29-day-old treated $Tk2^{KO}$ mice (Fig. 7A). Nonetheless, as untreated or PBS-

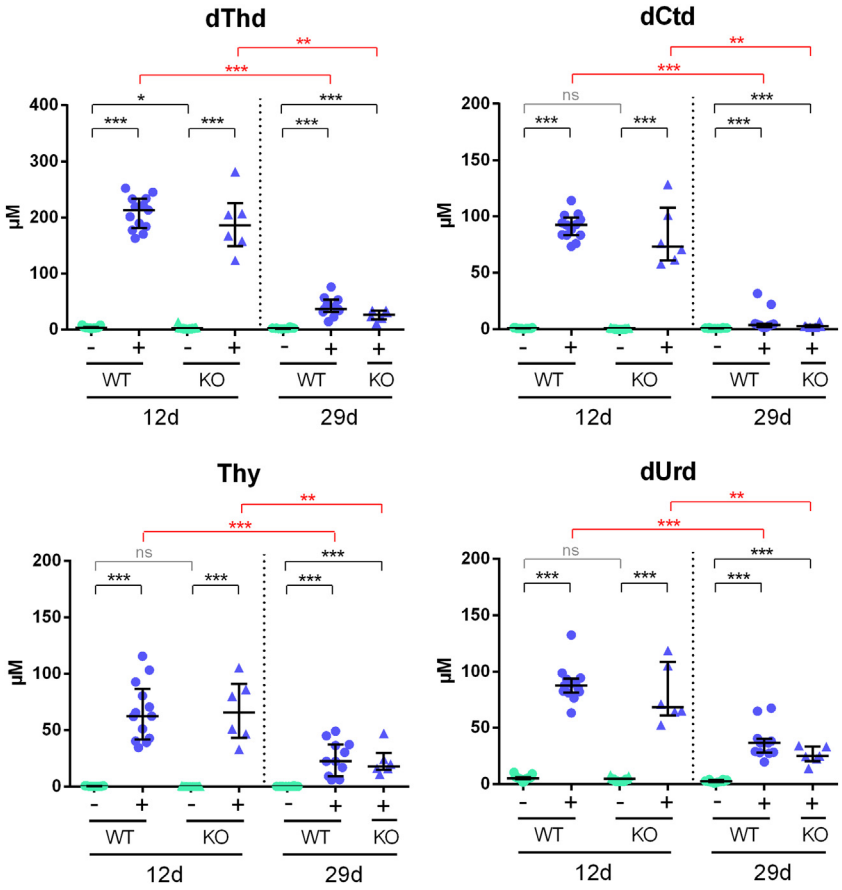

Fig. 4. Bioavailability of administered dThd + dCtd descreases with age. Concentrations of dThd, dCtd and their first degradation products (dUrd and Thy) in plasma of mice aged 12 (12d) or 29 days (29d) by LC-MS/MS. Results indicate metabolite concentrations (μM) in plasma of *Tk2*^{KO} (KO; triangles) and *Tk2*^{WT} (WT; dots) mice, treated with either 400 mg/kg/day of dThd +dCtd (+; blue) or PBS (−; green). Blood was collected 1 h after oral gavage. Scatter plots represent the median (horizontal line) with interquartile range (12d: *Tk2*^{WT}-PBS, $n = 13$; *Tk2*^{WT}-dThd+dCtd, n = 13; *Tk2*^{KO}-PBS, $n = 17$; *Tk2*^{KO}-dThd+dCtd, $n = 6$. 29d: *Tk2*^{WT}-PBS, $n = 10$; *Tk2*^{WT}-dThd+dCtd, n = 11; *Tk2*^{KO}-dThd+dCtd, n = 6). *P*-values obtained with the Mann-Whitney *U* test: ***p < .001; ns, non-significant differences. Age-related statistical significance lines and *p*-values are in red.

treated *Tk2*^{KO} are not viable after 20 days of life [34], we cannot exclude a contribution of chronic daily dThd+dCtd administration to these observations.

3.5. dThd alone is responsible for the therapeutic effect

Even though the two dNs were administered at the same dose, we systematically observed lower bioavailability for dCtd than for dThd (Figs. 4 and 5). This observation prompted us to investigate the contribution of each dN to the therapeutic effect. To this end, we administered dThd or dCtd to independent groups of *Tk2*^{KO} and *Tk2*^{WT} littermates. Administration of 400 mg/kg/day dCtd had no effect on the lifespan of *Tk2*^{KO} (median, 15 days of age; mean ± SD, 17.7 ± 1.5 days of age; $n = 6$), but administration of the same dose of dThd increased life expectancy to a median of 33 days (mean ± SD, 34.2 ± 2.6 days of age; $n = 12$), similar to the values obtained after combined administration of dThd+dCtd at the same dose (Fig. 8A). In addition, the body weight evolution in dThd-treated *Tk2*^{KO} was equivalent to that observed with the combined treatment (Fig. 8B).

In light of these results, we proceeded to investigate bioavailability and mtDNA copy number in a group of animals given only dThd (400 mg/kg/day). We found that plasma dThd concentration was around two-fold higher in these animals than in those administered dThd +dCtd at the same dose (Figs. 4 and 9). A mild increase in dUrd plasma concentration occurred in parallel to the increased bioavailability of dThd (Fig. 9), likely because of substrate competition between dThd and dUrd for TP activity. We observed a similar relative increase for dThd and Thy concentration in brain and skeletal muscle of dThd-treated mice. However, in small intestine and liver, either dThd or Thy concentrations were equivalent in some groups to those achieved after combined administration of dThd+dCtd (Supplementary Fig. 5). In contrast, acute oral administration of the same dose of dCtd alone resulted in concentrations similar to those found in animals receiving the combined therapy (Supplementary Fig. 6).

Analysis of mtDNA copy number in brain, liver and small intestine evidenced a better response after administration of dThd alone than when combined with dCtd (Fig. 9B and Fig. 3). In general, all groups of mice experienced a greater increase in mtDNA copy number after dThd administration, including *Tk2*^{WT} mice (Fig. 9B).

Importantly, mtDNA copy number nearly normalized in brain of 12-day-old *Tk2*^{KO} animals treated with dThd only, whereas the combined treatment induced no positive response in this tissue. However, in skeletal muscle of mice at the same age, a better response was achieved after combined dThd+dCtd administration (Fig. 9B). These findings suggest that complex tissue-specific metabolic regulations may affect the outcome of dN-based therapies.

At a later stage, 29-days of age, liver, brain and especially skeletal muscle, experience a marked increase in mtDNA copy number as part of their normal development (as indicated by the increase observed in *Tk2*^{WT} mice). At this timepoint, no treatment was able to normalize mtDNA levels.

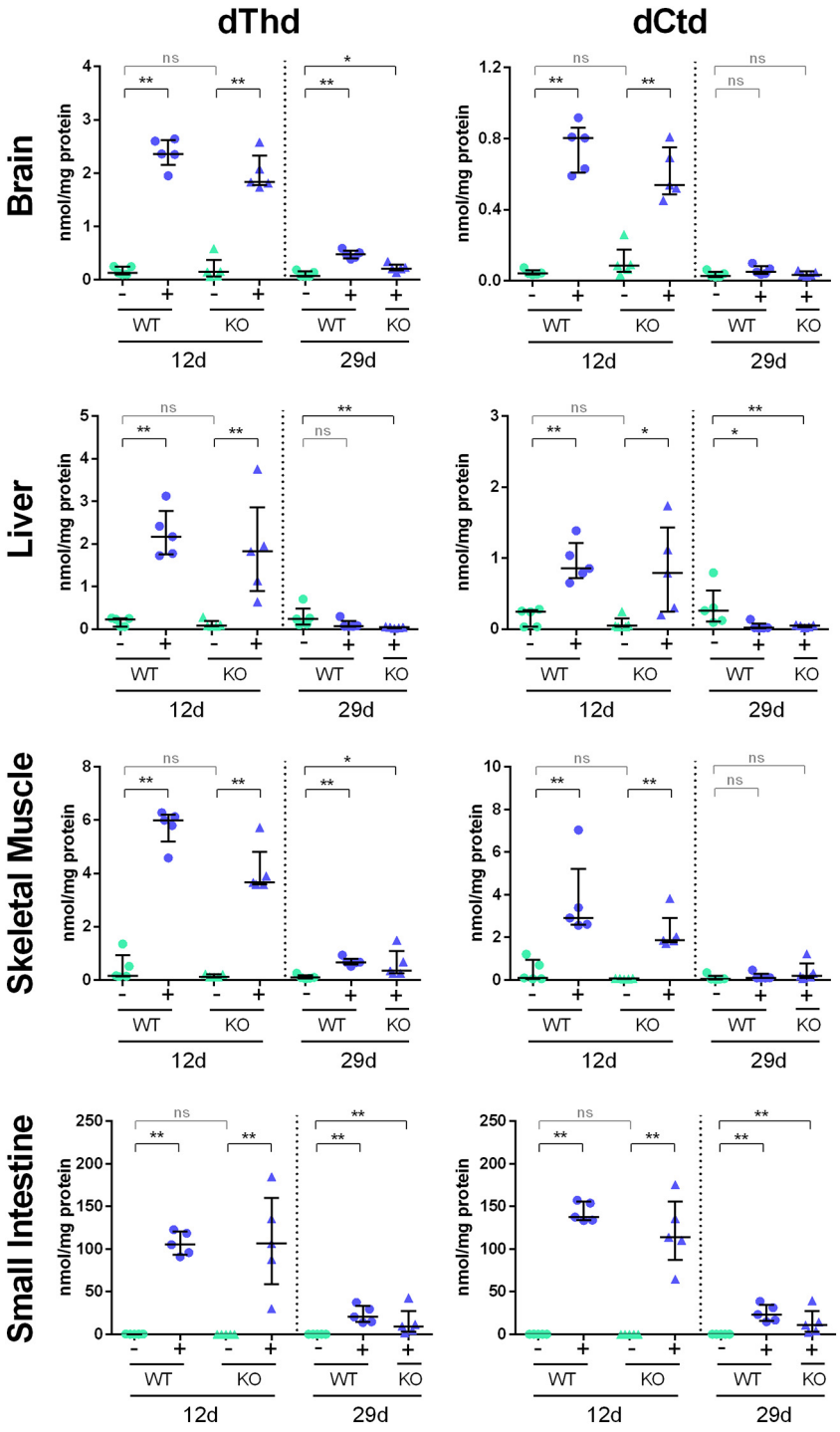

Fig. 5. dThd and dCtd concentrations in tissues are lower in older mice. dThd and dCtd concentrations in brain, liver, skeletal muscle (gastrocnemius), and small intestine determined by LC-MS/MS. Results are expressed in nmols per mg of protein in tissues of mice aged 12 (12d) or 29 days (29d). $Tk2^{KO}$ (KO; triangles) and $Tk2^{WT}$ (WT; dots) mice, treated with either 400 mg/kg/day of dThd+dCtd (+; blue) or PBS (−; green). Tissues were collected 1 h after oral gavage. Scatter plots represent the median (horizontal line) with interquartile range. Mice in each group, $n = 5$. P-values obtained with the Mann-Whitney U test: $^{*}p < .05$; $^{**}p < .01$; ns, non-significant differences.

4. Discussion

Previous studies had shown that dN supplementation delays disease progression and expands survival in a knockin mouse model for the p.His121Asn mutation [10,16]. However, kinetic studies revealed that the mutant protein retains its capacity for dThd phosphorylation, suggesting that increased substrate concentration might stimulate residual enzyme activity [31]. The fact that dThd+dCtd administration has a similar effect on a knockout model devoid of any TK2 enzyme activity [34] as was shown here, leads to the conclusion that dNs must recruit alternative pathways for their ultimate transformation into dNTPs. This would imply that this type of therapy may be effective for any TK2 pathogenic mutation whether or not there is any residual enzyme activity.

Although we observed a notable effect on survival, which doubled with dThd+dCtd treatment, $Tk2^{KO}$ mice still exhibited growth retardation and prematurely died before adulthood (median survival, 34 days). Thus, the therapy delays disease progression but fails to completely rescue the phenotype in mice. In an attempt to uncover

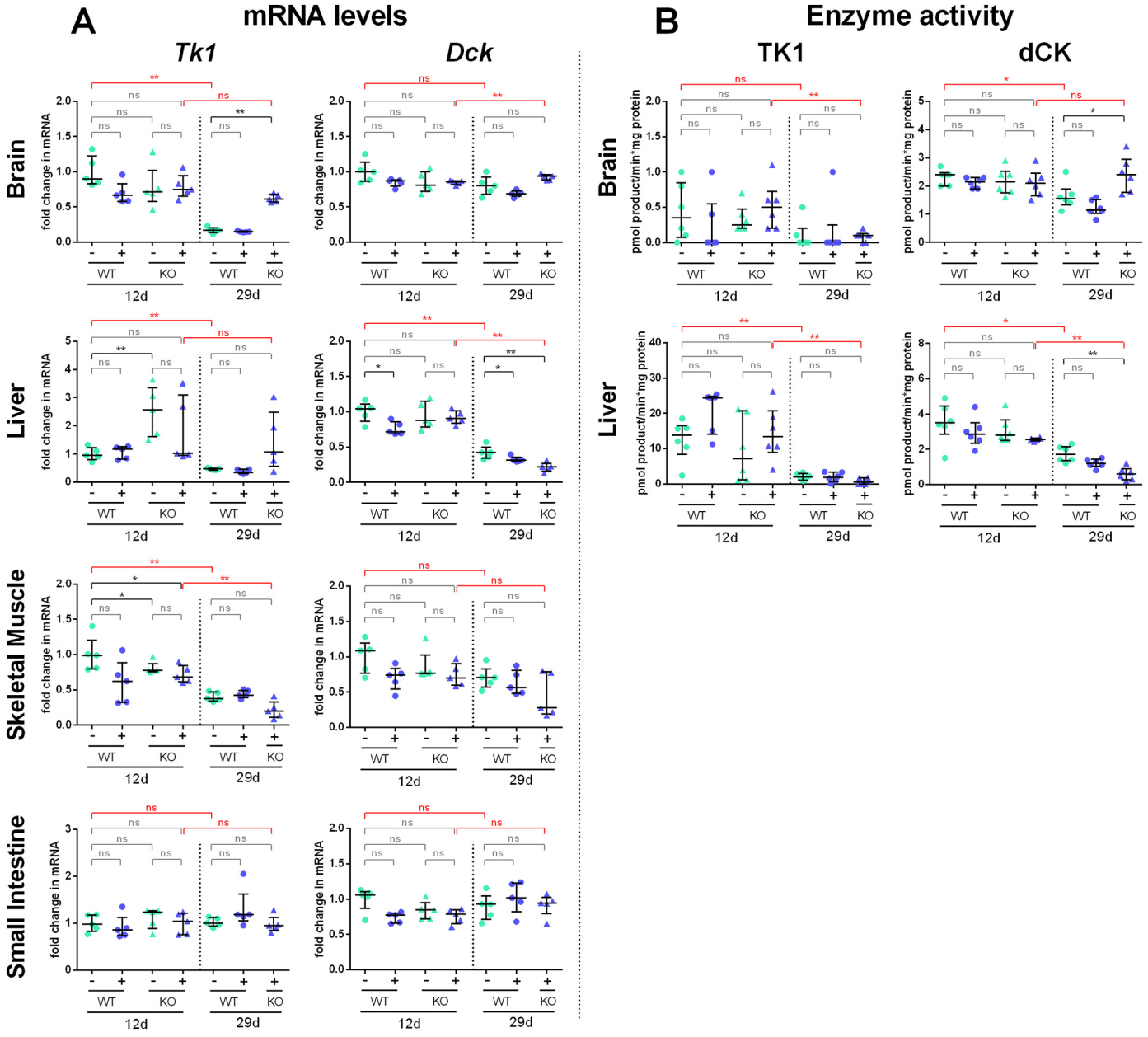

Fig. 6. dN anabolic enzyme mRNA expression and activity decrease during mouse development. We measured mRNA levels and enzyme activity of cytosolic salvage kinases involved in dThd and dCtd activation (TK1 and dCK, respectively) in various targeted tissues from mice aged 12 (12d) or 29 days (29d). Tissues were collected 1 h after oral gavage. Scatter plots represent the median (horizontal line) with interquartile range. P-values obtained with the Mann-Whitney U test: *p < .05; **p < .01; ns, non-significant differences. (**A**) Relative *Tk1* and *Dck* mRNA levels in brain, liver, skeletal muscle (gastrocnemius), and small intestine, determined by real-time PCR with specific TaqMan probes. *Ppia* mRNA level was used for normalization between samples. Results are represented as the fold change related to the mean value in 12-day-old PBS-treated $Tk2^{WT}$ mice. Mice in each group, $n = 5$. (**B**) TK1 and dCK enzyme activities in brain and liver, determined using a biochemical method with specific radiolabelled substrates. Results are represented as pmol of product formed in 1 min from 1 mg of protein in tissue homogenate. Mice in each group, $n = 6$. Age-related statistical significance lines and p-values are in red.

factors that could be critical in limiting the effectiveness of dNs, we identified ontogenetic changes in the expression of related catabolic enzymes and necessary cytosolic salvage kinases. dThd and dCtd bioavailability was clearly reduced in older mice. The activity of CDA and principally TP, which catalyse the first degradation step of dCtd and dThd, respectively, was markedly increased in small intestine of older mice, a decisive tissue for the bioavailability of orally administered substances. Accordingly, in tissues of older mice, the decrease in dThd and dCtd levels was generally larger than that of their respective catabolic products, in agreement with higher degradation activities. Other routes of administration, such as intraperitoneal (IP) injection leads to higher bioavailability of dThd+dCtd. However, IP administration of dThd+dCtd to a TK2 His126Asn knockin mouse model yielded similar results on survival [17], so reduced efficacy of deoxynucleosides with aging is likely due to factors other than simply absorption at the level of small intestine. The activity of the required cytosolic deoxynucleoside kinases (TK1 and dCK) was also markedly altered with age, especially in brain and liver where both activities were significantly reduced, which could also contribute to the age-related loss of effect. Overall, our findings regarding these limiting factors are in agreement with the observations on a TK2 His126Asn knockin mice after IP and oral dThd+dCtd administration [16,17]. Finally, ontogenetic changes in other factors, such as dN transporters involved in intestinal absorption and cellular internalization, could further lessen the therapeutic potential of dNs in older mice.

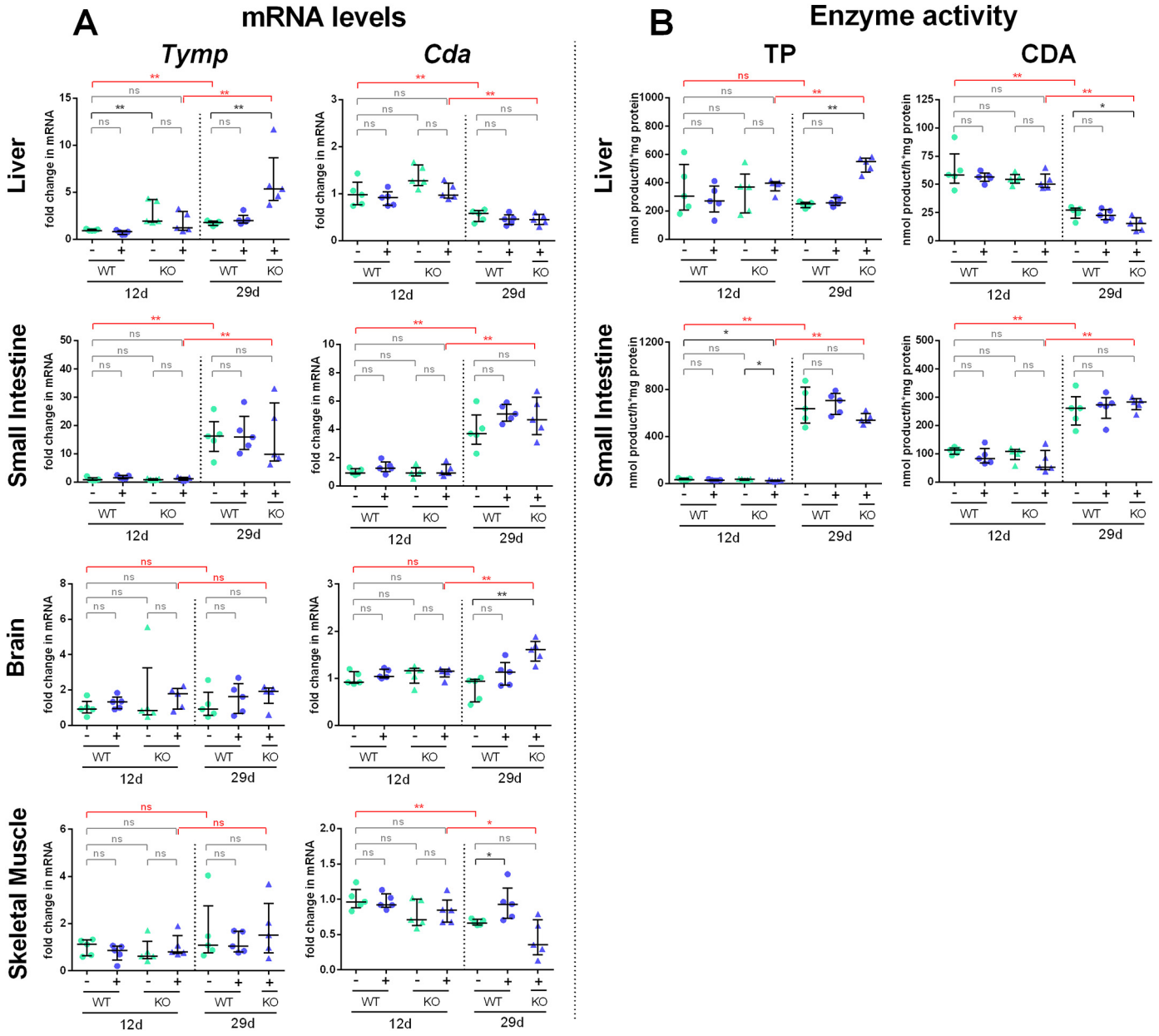

Fig. 7. dNs catabolic enzyme mRNA expression and activity is upregulated in small intestine of older mice. mRNA levels and enzyme activity of the main catabolic enzymes involved in dThd and dCtd degradation (TP and CDA, respectively) in various target tissues of mice aged 12 (12d) or 29 days (29d). Tissues were collected 1 h after oral gavage. Scatter plots represent the median (horizontal line) with interquartile range. *P*-values obtained with the Mann-Whitney *U* test: $^{*}p < .05$; $^{**}p < .01$; ns, non-significant differences. (**A**) Relative *Tymp* and *Cda* mRNA levels of in brain, liver, skeletal muscle (gastrocnemius), and small intestine determined by real-time PCR with specific TaqMan probes. *Ppia* mRNA level was used for normalization between samples. Results are represented as the fold change relative to the mean value in 12-day-old PBS-treated $Tk2^{WT}$ mice. Mice in each group, $n = 5$. (**B**) TP and CDA enzyme activities, determined by a biochemical method coupled to UPLC analysis in liver and small intestine. Results are represented as nmol of product formed in 1 h from 1 mg of protein in tissue homogenate. Mice in each group, n = 5. Age-related statistical significance lines and p-values are in red.

In addition, important tissue-specific differences were evident already at early ages. As an example, while mtDNA was repopulated in skeletal muscle of young treated $Tk2^{KO}$ mice in response to combined administration of dThd and dCtd, the same treatment triggered no detectable increase in mtDNA copy number in brain, another targeted tissue. dNs can cross the blood-brain barrier through the activity of dedicated transporters [23,28]. Accordingly, our results showed a marked increase in brain dN concentrations already 1 h after administration, suggesting that lack of effectiveness depends on downstream events, such as the extremely low TK1 activity detected in this tissue which makes it more dependent on TK2 activity [7,27].

Interestingly, although TK2 is responsible for both dThd and dCtd phosphorylation in mitochondria, we found that the therapeutic effect of the combined therapy on survival in mice actually depends on dThd alone. Non-dividing cells are highly dependent on deoxynucleoside salvage due to downregulation of de novo dNTP synthesis pathways (Fig. 1). Unlike dCK, which is ubiquitously expressed throughout cell cycle, TK1 expression is highly linked to S-phase during cell cycle [13,22]. Thus, mtDNA synthesis demands for dCTP are possibly lower than for dTTP in the absence of functional TK2 activity. In fact, administration only of dThd led to a higher mtDNA repopulation index in most tissues of 12-day-old mice, including brain, in which levels were much closer to normalization than after dThd plus dCtd co-administration. This effect is consistent with the finding of higher plasma and tissue dThd concentration after administration of dThd alone, which is likely due to interactions of both these pyrimidine dNs with transporters

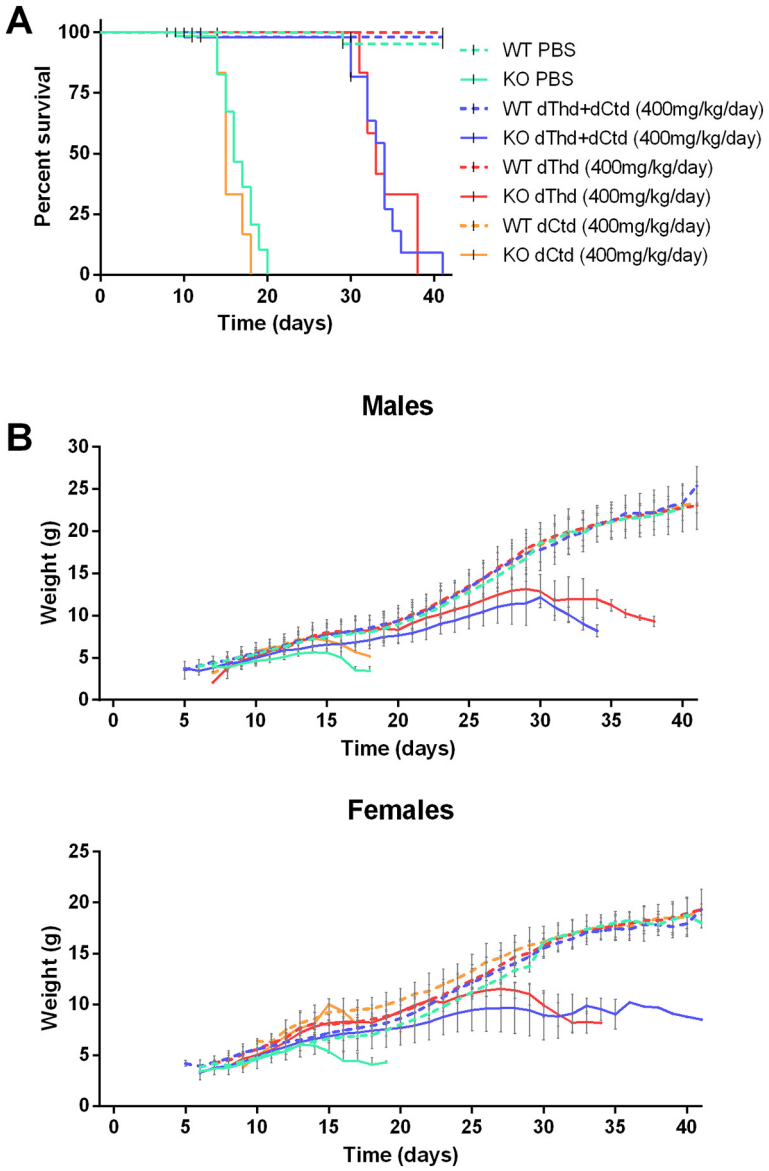

Fig. 8. dThd is responsible for extended survival and slowed disease progression. in $Tk2^{KO}$ mice. $Tk2^{KO}$ mice (solid lines) and $Tk2^{WT}$ (dashed lines) littermates were daily administered PBS (vehicle; 10 μl/g; green lines), 400 mg/kg of dThd+dCtd (blue lines), 400 mg/kg of dCtd (orange lines) or 400 mg/kg of dThd (red lines). PBS and dThd+dCtd treated mice were included also in Fig. 1. (**A**) Survival proportions, Kaplan-Meier curve ($Tk2^{WT}$-dThd, $n = 10$; $Tk2^{KO}$-dThd, $n = 12$; $Tk2^{WT}$-dCtd, $n = 9$; $Tk2^{KO}$-dCtd, n = 6. Mantel-Cox test: $Tk2^{KO}$-PBS versus $Tk2^{KO}$-dThd $p < .001$; $Tk2^{KO}$-dThd versus $Tk2^{KO}$-dThd+dCtd no significant differences; $Tk2^{KO}$-dThd+dCtd versus $Tk2^{KO}$-dCtd $p < .001$; $Tk2^{KO}$-PBS versus $Tk2^{KO}$-dCtd; ns, non-significant differences). Censored observations appear as black ticks in the graph (**B**) Growth progression for female and male mice (Males: $Tk2^{WT}$-dThd, n = 9; $Tk2^{KO}$-dThd, n = 12; $Tk2^{WT}$-dCtd, $n = 8$; $Tk2^{KO}$-dCtd, $n = 3$. Females: $Tk2^{WT}$-dThd, n = 10; $Tk2^{KO}$-dThd, n = 5; $Tk2^{WT}$-dCtd, n = 3; $Tk2^{KO}$-dCtd, $n = 4$. Results represent mean values for each time point; error bars indicate SD).

involved in their absorption [21]. The positive mtDNA synthesis response in brain provides evidence that the extremely low TK1 levels in this tissue can still be stimulated by high concentrations of substrate, (ie, dThd), a particularly relevant finding from the standpoint of therapeutic effectiveness, and is another indication that reduced availability of dNs with age may be an important limitation to this therapy.

In contrast to what occurs in humans, who mainly manifest TK2 deficiency as a purely myopathic condition [11,25], mice show marked CNS involvement [1,3,34]. Thus, the ability of dThd to repopulate mtDNA in brain appeared to be a key factor defining the effectiveness of this treatment in mice. Nevertheless, survival after dThd administration alone was equivalent to survival after the combined therapy. Up-regulation of catabolic enzymes, and particularly of TP, at a later age leads to lower dThd concentrations in plasma and lower mtDNA repopulation in all target tissues, which possibly leads to ultimately equivalent effects on survival than after the combined therapy of dThd+dCtd.

Taken together, our results would seem to argue against any need for dCtd, as it apparently provided no benefits over dThd alone in mice. However, the dCtd increase after treatment was smaller than that of dThd already at early stages of development. Thus, we cannot rule out the possibility that a positive response might be triggered in $Tk2^{KO}$ mice by increasing dCtd availability. Furthermore, although higher dThd availability led to better results in brain, it had a detrimental effect on mtDNA copy number in skeletal muscle of young $Tk2^{KO}$ mice, indicating that demands for the different dNTP species may vary between the various target tissues. A similar observation has been made by López-Gómez et al. in liver from older TK2-deficient mice [17]. Such tissue-specific metabolic requirements and homeostasis make it difficult to define the contribution of each particular tissue to the therapeutic intervention and to the overall disease phenotype. In addition, other mouse models for dNTP metabolism-related defects display phenotypes that are remarkably different from those in humans

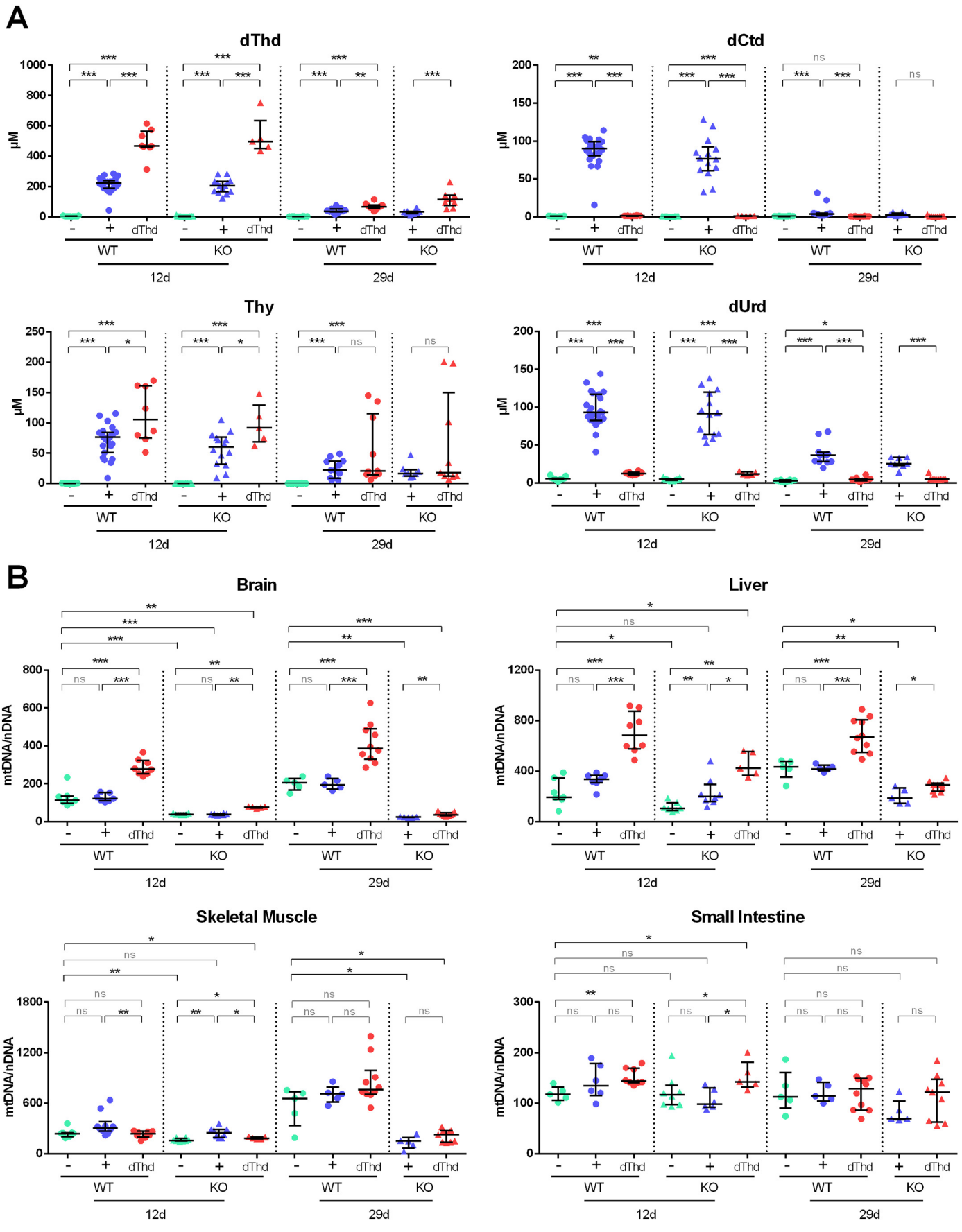
A
dThd
dCtd
Thy
dUrd
µM
B
Brain
Liver
Skeletal Muscle
Small Intestine
mtDNA/nDNA
WT
KO
12d
29d
dThd
ns

[5,18], suggesting considerable divergence in dNTP homeostasis between the two species. All these observations prevent us from anticipating whether dCtd administration may be dispensable in humans, where muscle is actually the main tissue affected.

Other issues should also be considered when analysing factors with a potential impact on therapy efficacy. It is possible that a lack of TK2 activity could trigger some adaptive changes that would be detected as genotype-linked differences. Nonetheless, we detected scarce differences between genotypes at day 12 of age, and on day 29, the observations were challenged by the absence of PBS-treated *Tk2*^{KO} mice, which did not survive beyond day 20. Also, animals were exposed to daily treatment starting from postnatal day 4. Thus, we cannot exclude that our observations in *Tk2*^{KO} mice on day 29 may be due to the combined effect of chronic exposure to treatment and genotype adaptations. For example, we observed higher *Dck* and *Cda* mRNA levels in brain of *Tk2*^{KO}. Liver TP activity, and consequently Thy levels, were also higher, specifically in *Tk2*^{KO} mice. In agreement with this observation, we found that concentrations of dThd and dUrd, both substrates of TP, were lower in various tissues of treated *Tk2*^{KO} (Figs. 4 and 5 and Supplementary Fig. 1).

Garone et al. reported an increase in TK1 activity after chronic dTMP and dCMP administration [10]. We found that *Tk1* mRNA levels, which normally drop with age, were sustained in brain from treated *Tk2*^{KO} mice (Fig. 6A). This interesting result suggests that the high dThd levels could stabilise TK1 by increasing *TK1* transcription. In fact, although TK1 undergoes specific proteolysis in mitotic exit, dThd binding to TK1 has been shown to stabilise the enzyme during growth arrest in HeLa cells [14]. However, our activity measurements did not corroborate our mRNA observations, which suggest a participation of posttranslational degradation mechanisms that would counteract upregulation of *TK1* transcription [13]. Furthermore, it is important to note that 29-day-old *Tk2*^{KO} mice are at a late stage of the disease, so some of the effects observed may be associated with this circumstance.

TK2 deficiency reduces dTTP and dCTP levels, interfering with mtDNA replication. By activating alternative salvage pathways, the treatment provided enough substrates to counteract mtDNA depletion in most tissues from young *Tk2*^{KO} mice. In addition, increased dThd concentration also led to increased mtDNA levels in treated *Tk2*^{WT} mice. In *Tk2*^{WT}, expansion of the mitochondrial dTTP pool counts on functional TK2 activity in addition to cytosolic salvage. In fact, the increase in mtDNA levels was higher in some tissues of *Tk2*^{WT} than of *Tk2*^{KO} mice (Fig. 9). These results suggest that basal dNTP levels, actually limit mtDNA replication in normal physiological conditions, at least in some tissues.

Unbalanced dNTP pools may have detrimental consequences for DNA replication fidelity [20]. Mutation frequencies in nuclear and mitochondrial genome seemed not affected in transgenic *Tk2*^{KO} mice overexpressing cytosolic *DmdNK*, which lead to a 200-fold and 5-fold expansion of dTTP and dCTP pools respectively [15]. Nevertheless, mutagenesis and other dN therapy-related safety issues will necessarily be addressed in further research.

Despite the significant differences between humans and mice regarding dNTP homeostasis, we believe the results of this study provide insight into the pathomechanisms underlying TK2 deficiency and offer useful information on key factors that could limit the efficacy of dNs-based therapies. These data are of value, as dNs are currently being applied in clinical use in TK2-deficient patients [6], and they will be of interest in the design of an upcoming clinical trial.

Acknowledgements

We wish to thank the patients and their families for their collaboration in this study. We also thank Dr. José Luis Martínez Moreno and José Julián Martínez Padilla for their helpful insight when developing the project, Dr. Liya Wang for crucial technical advice on enzyme activity determinations, and Dr. Michio Hirano and Dr. Carlos López (Columbia University, NY) for fruitful cooperative discussions throughout the project.

Funding sources

This study was funded by grants from the Spanish Ministry of Industry, Economy and Competitiveness [grant BFU2014-52618-R and SAF2017-87506-R to YC], the Spanish Instituto de Salud Carlos III [grant PI15/00465 and grant PMP 15/00025 to RM, co-financed with ERDF], the Fundación Inocente, Inocente [grant 2017 to YC], and AFM Téléthon [grant 19,965 to YC]. JT was funded by a fellowship granted by the Generalitat de Catalunya (PERIS program, SLT002/16/00370). The disclosed funders had no role in study design, data collection and analysis, decision to publish, or preparation of the manuscript.

Declaration of interests

RM and the Vall d'Hebron Research Institute (VHIR) have filed patent applications covering potential use of deoxythymidine and deoxycytidine treatment for TK2 deficiency in humans. RM, YC, CB, JT, VHIR and The Biomedical Network Research Centre on Rare Diseases (CIBERER) have filed patent applications covering potential use of deoxynucleoside treatment for POLG deficiency and other mtDNA replication defects in humans. VHIR and CIBERER have licensed pending patent applications related to these technologies to MODIS Therapeutics, Inc., and VHIR and CIBERER may be eligible to receive payments related to the development and commercialization of the technologies. Any potential licensing fees earned will be paid to VHIR and CIBERER and are shared with all inventors mentioned above through VHIR and CIBERER policies on distribution and objectivity in research. RM serves as a paid consultant to MODIS Therapeutics, Inc. and has equity in this company. RM, YC, CB, VHIR and The Biomedical Network Research Centre on Rare Diseases (CIBERER) have filed patent applications covering potential use of deoxynucleoside treatment as a way to increase mtDNA copy number.

Authors contribution

C. Blázquez-Bermejo, R. Martí, and Y. Cámara designed the study; C. Blázquez-Bermejo, D. Molina-Granada, F. Vila-Julià, D. Jiménez-Heis J. Torres-Torronteras, R. Martí and Y. Cámara performed experiments, collected and analysed the data; X. Zhou and A. Karlsson generated the TK2-knockout mouse model, actively participated in project discussions and contributed to data analysis; C. Blázquez-Bermejo and Y. Cámara wrote the manuscript; All contributing authors participated in the critical reading of the manuscript; Y.Cámara supervised the project, had full

Fig. 9. Higher dThd concentration correlates with higher mtDNA copy number in targeted tissues. Concentration of metabolites in plasma and mtDNA copy number in tissues of mice aged 12 (12d) or 29 days (29d) and of *Tk2*^{KO} (KO; triangles) or *Tk2*^{WT} (WT; dots) mice, treated with either 400 mg/kg/day of dThd+dCtd (+; blue), dThd (dThd, red), or PBS (−; green). Tissues and blood were collected 1 h after oral gavage. Scatter plots represent the median (horizontal line) with interquartile range. P-values obtained with the Mann-Whitney U test: *p < .05; **p < .01; ***p < .001; ns, non-significant differences. (**A**) Concentration (μM) of dThd, Thy, dCtd and dUrd in plasma, assessed by LC-MS/MS (12d:*Tk2*^{WT}-PBS, *n* = 13; *Tk2*^{WT}-dThd+dCtd, *n* = 23; *Tk2*^{WT}-dThd, n = 8; *Tk2*^{KO}-PBS, *n* = 17; *Tk2*^{KO}-dThd+dCtd, *n* = 14; *Tk2*^{KO}-dThd, n = 5. 29d: *Tk2*^{WT}-PBS, n = 10; *Tk2*^{WT}-dThd+dCtd, *n* = 11; *Tk2*^{WT}-dThd, n = 10; *Tk2*^{KO}-dThd+dCtd, n = 8; *Tk2*^{KO}-dThd, n = 9). (**B**) mtDNA and nDNA levels were determined by quantitative real-time PCR. Results indicate the ratio of mtDNA to nDNA in brain, liver, skeletal muscle (gastrocnemius), and small intestine (mice in each group in brain, n = 5–10; liver, n = 5–10; skeletal muscle, n = 5–10 and small intestine, n = 5–10).

access to data in the study and had final responsibility for the decision to submit for publication.

Appendix A. Supplementary data

Supplementary data to this article can be found online at https://doi.org/10.1016/j.ebiom.2019.07.042.

References

[1] Akman HO, Dorado B, Lopez LC, Garcia-Cazorla A, Vila MR, Tanabe LM, et al. Thymidine kinase 2 (H126N) knockin mice show the essential role of balanced deoxynucleotide pools for mitochondrial DNA maintenance. Hum Mol Genet 2008;17:2433–40.

[2] Alston CL, Schaefer AM, Raman P, Solaroli N, Krishnan KJ, Blakely EL, et al. Late-onset respiratory failure due to TK2 mutations causing multiple mtDNA deletions. Neurology 2013;81:2051–3.

[3] Bartesaghi S, Betts-Henderson J, Cain K, Dinsdale D, Zhou X, Karlsson A, et al. Loss of thymidine kinase 2 alters neuronal bioenergetics and leads to neurodegeneration. Hum Mol Genet 2010;19:1669–77.

[4] Camara Y, Gonzalez-Vioque E, Scarpelli M, Torres-Torronteras J, Caballero A, Hirano M, et al. Administration of deoxyribonucleosides or inhibition of their catabolism as a pharmacological approach for mitochondrial DNA depletion syndrome. Hum Mol Genet 2014;23:2459–67.

[5] Dalla Rosa I, Camara Y, Durigon R, Moss CF, Vidoni S, Akman G, et al. MPV17 loss causes deoxynucleotide insufficiency and slow DNA replication in mitochondria. PLoS Genet 2016;12:e1005779.

[6] Dominguez-Gonzalez C, Madruga-Garrido M, Mavillard F, Garone C, Aguirre-Rodriguez FJ, Donati MA, et al. Deoxynucleoside therapy for thymidine kinase 2 (TK2) deficient myopathy. Ann Neurol 2019;86:293–303.

[7] Dorado B, Area E, Akman HO, Hirano M. Onset and organ specificity of Tk2 deficiency depends on Tk1 down-regulation and transcriptional compensation. Hum Mol Genet 2011;20:155–64.

[8] el Kouni MH, el Kouni MM, Naguib FN. Differences in activities and substrate specificity of human and murine pyrimidine nucleoside phosphorylases: implications for chemotherapy with 5-fluoropyrimidines. Cancer Res 1993;53:3687–93.

[9] Fanucchi MP, Watanabe KA, Fox JJ, Chou TC. Kinetics and substrate specificity of human and canine cytidine deaminase. Biochem Pharmacol 1986;35:1199–201.

[10] Garone C, Garcia-Diaz B, Emmanuele V, Lopez LC, Tadesse S, Akman HO, et al. Deoxypyrimidine monophosphate bypass therapy for thymidine kinase 2 deficiency. EMBO Mol Med 2014;6:1016–27.

[11] Garone C, Taylor RW, Nascimento A, Poulton J, Fratter C, Dominguez-Gonzalez C, et al. Retrospective natural history of thymidine kinase 2 deficiency. J Med Genet 2018;55:515–21.

[12] Gotz A, Isohanni P, Pihko H, Paetau A, Herva R, Saarenpaa-Heikkila O, et al. Thymidine kinase 2 defects can cause multi-tissue mtDNA depletion syndrome. Brain 2008;131:2841–50.

[13] Hu CM, Chang ZF. Mitotic control of dTTP pool: a necessity or coincidence? J Biomed Sci 2007;14:491–7.

[14] Ke PY, Hu CM, Chang YC, Chang ZF. Hiding human thymidine kinase 1 from APC/C-mediated destruction by thymidine binding. FASEB J 2007;21:1276–84.

[15] Krishnan S, Paredes JA, Zhou X, Kuiper RV, Hultenby K, Curbo S, et al. Long term expression of Drosophila melanogaster nucleoside kinase in thymidine kinase 2-deficient mice with no lethal effects caused by nucleotide pool imbalances. J Biol Chem 2014;289:32835–44.

[16] Lopez-Gomez C, Levy RJ, Sanchez-Quintero MJ, Juanola-Falgarona M, Barca E, Garcia-Diaz B, et al. Deoxycytidine and Deoxythymidine treatment for thymidine kinase 2 deficiency. Ann Neurol 2017;81:641–52.

[17] Lopez-Gomez C, Hewan H, Sierra C, Akman HO, Sanchez-Quintero MJ, Juanola-Falgarona M, et al. Bioavailability and activities of cytosolic kinases modulate response to deoxynucleoside therapy in TK2 deficiency. Submitted 2019;2019.

[18] Lopez LC, Akman HO, Garcia-Cazorla A, Dorado B, Marti R, Nishino I, et al. Unbalanced deoxynucleotide pools cause mitochondrial DNA instability in thymidine phosphorylase-deficient mice. Hum Mol Genet 2009;18:714–22.

[19] Marti R, Lopez LC, Hirano M. Assessment of thymidine phosphorylase function: measurement of plasma thymidine (and deoxyuridine) and thymidine phosphorylase activity. Methods Mol Biol 2012;837:121–33.

[20] Mathews CK. DNA precursor metabolism and genomic stability. FASEB J 2006;20:1300–14.

[21] Pastor-Anglada M, Urtasun N, Perez-Torras S. Intestinal nucleoside transporters: function, expression, and regulation. Compr Physiol 2018;8:1003–17.

[22] Rampazzo C, Miazzi C, Franzolin E, Pontarin G, Ferraro P, Frangini M, et al. Regulation by degradation, a cellular defense against deoxyribonucleotide pool imbalances. Mutat Res 2010;703:2–10.

[23] Redzic ZB, Malatiali SA, Grujicic D, Isakovic AJ. Expression and functional activity of nucleoside transporters in human choroid plexus. Cerebrospinal Fluid Res 2010;7(2).

[24] Rylova SN, Mirzaee S, Albertioni F, Eriksson S. Expression of deoxynucleoside kinases and 5′-nucleotidases in mouse tissues: implications for mitochondrial toxicity. Biochem Pharmacol 2007;74:169–75.

[25] Saada A, Shaag A, Mandel H, Nevo Y, Eriksson S, Elpeleg O. Mutant mitochondrial thymidine kinase in mitochondrial DNA depletion myopathy. Nat Genet 2001;29:342–4.

[26] Saada A, Ben-Shalom E, Zyslin R, Miller C, Mandel H, Elpeleg O. Mitochondrial deoxyribonucleoside triphosphate pools in thymidine kinase 2 deficiency. Biochem Biophys Res Commun 2003;310:963–6.

[27] Saada A, Shaag A, Elpeleg O. mtDNA depletion myopathy: elucidation of the tissue specificity in the mitochondrial thymidine kinase (TK2) deficiency. Mol Genet Metab 2003;79:1–5.

[28] Spector R, Eells J. Deoxynucleoside and vitamin transport into the central nervous system. Fed Proc 1984;43:196–200.

[29] Tyynismaa H, Sun R, Ahola-Erkkila S, Almusa H, Poyhonen R, Korpela M, et al. Thymidine kinase 2 mutations in autosomal recessive progressive external ophthalmoplegia with multiple mitochondrial DNA deletions. Hum Mol Genet 2012;21:66–75.

[30] Walker UA, Auclair M, Lebrecht D, Kornprobst M, Capeau J, Caron M. Uridine abrogates the adverse effects of antiretroviral pyrimidine analogues on adipose cell functions. Antivir Ther 2006;11:25–34.

[31] Wang L, Saada A, Eriksson S. Kinetic properties of mutant human thymidine kinase 2 suggest a mechanism for mitochondrial DNA depletion myopathy. J Biol Chem 2003;278:6963–8.

[32] Wang L. Mitochondrial purine and pyrimidine metabolism and beyond. Nucleosides Nucleotides Nucleic Acids 2016;35:578–94.

[33] Young JD. The SLC28 (CNT) and SLC29 (ENT) nucleoside transporter families: a 30-year collaborative odyssey. Biochem Soc Trans 2016;44:869–76.

[34] Zhou X, Solaroli N, Bjerke M, Stewart JB, Rozell B, Johansson M, et al. Progressive loss of mitochondrial DNA in thymidine kinase 2-deficient mice. Hum Mol Genet 2008;17:2329–35.

[35] Zimmermann H, Zebisch M, Strater N. Cellular function and molecular structure of ecto-nucleotidases. Purinergic Signal 2012;8:437–502.